UC Berkeley
UC Berkeley Previously Published Works

Title

Seismic earth pressures on retaining structures and basement walls in cohesionless soils

Permalink

https://escholarship.org/uc/item/2nz3b9m7

Journal

Journal of Geotechnical and Geoenvironmental Engineering, 142(10)

ISSN

1090-0241

Authors

Mikola, RG
Candia, G
Sitar, N

Publication Date

2016-10-01

DOI

10.1061/(ASCE)GT.1943-5606.0001507

Peer reviewed

Seismic Earth Pressures on Retaining Structures and Basement Walls in Cohesionless Soils

Roozbeh Geraili Mikola, Ph.D., P.E.[1]; Gabriel Candia, Ph.D., P.E.[2]; and Nicholas Sitar, Ph.D., P.E., M.ASCE[3]

[1] Project Engineer, McMillen Jacobs Associates, 49 Stevenson St., San Francisco, CA 94105 (corresponding author). E-mail: mikola@mcmjac.com [2] Professor, Facultad de Ingeniería Universidad del Desarrollo, National Research Center for Integrated Natural Disaster Management, CONICYT/ FONDAP/15110017, La Plaza 680, Las Condes, CP 7610658, Chile. E-mail: gcandia@udd.cl [3] Edward G. Cahill and John R. Cahill Professor, Dept. of Civil and Environmental Engineering, UC Berkeley, 449 Davis Hall UC Berkeley, Berkeley, CA 94720. E-mail: sitar@berkeley.edu

Abstract:

Observations of the performance of basement walls and retaining structures in recent earthquakes show that failures of basement or deep-excavation walls in earthquakes are rare even if the structures were not designed for the actual magnitude of the earthquake loading. For instance, no significant damage or failures of retaining structures occurred in the recent Wenchuan earthquake in China (2008) or in the subduction earthquakes in Chile (2010) and Japan (2011). To develop a better understanding of the distribution and magnitude of the seismic earth pressures on cantilever retaining structures, a series of centrifuge experiments were performed on model retaining and basement structures with medium dense cohesionless backfill. This paper provides a general overview of the research program and its results. Two sets of centrifuge-scale experiments were carried out on the centrifuge at the Center for Geotechnical Modeling at UC Davis. Three different types of prototype retaining structure were modeled in this research effort as follows: (1) a nondisplacing cross-braced (basement) structure with a stem stiffness of 5.92×10^{10} lb-in.^{2} per ft width (5.57×10^{05} kN-m^2 per m width) and 1.04×10^{10} lb-in.^{2} per ft width (9.79×10^{04} kN-m^2 per m width); (2) a nondisplacing U-shaped cantilever structure with a stem stiffness of 5.92 and 1.04×10^{10} lb-in.^{2} per ft width (9.79×10^{04} kN-m^2 per m width); and (3) a free standing, cantilever retaining wall with a stem stiffness of 2.4×10^{10} lb-in.^{2} per ft width (2.26×10^{05} kN-m^2 per m width). Overall, for the structures examined [i.e., wall heights in the range 6.1–9.15 m (20–30 ft)], the centrifuge data consistently show that the maximum dynamic earth pressure increases with depth and can be reasonably approximated by a triangular distribution. This suggests that the result of the dynamic earth pressure increment acts near $0.33H$ above the footing as opposed to 0.5–0.6 H recommended by most current design procedures. The current data also suggest that cantilever walls can resist ground accelerations up to 0.4 g if designed with an adequate static factor of safety.

Introduction

The problem of analyzing seismic earth pressures on retaining structures is complicated by the fact that it involves a dynamic soil-structure interaction that does not lend itself to easy simplification using limit equilibrium. Nevertheless, such simplification is the essence of the most commonly used limit equilibrium method of analysis, usually referred to as the Mononobe-Okabe (M-O) method, after the pioneering analyses and experiments carried out in Japan by Okabe (1924) and Mononobe and Matsuo (1929). Since then various researchers have addressed this problem to refine or modify the method of analysis (e.g., Seed and Whitman 1970; Nazarian and Hadjian 1979; Prakash and Basavanna 1969; Prakash 1981; Aitken 1982; Mylonakis et al. 2007). Nevertheless, with the exception of the simplification proposed by Seed and Whitman (1970), these efforts have had relatively little impact on design and engineering practice.

Sitar et al. (2012), in reviewing the state of practice, noted that in the United States the Uniform Building Code (UBC) did not contain provisions for seismic design of retaining structures until 2003, although the California Building Code (CBC) contained provisions for certain types of building walls going back to the 1980s (Lew et al. 2010b). However, with the recent reassessment of seismic hazard severity based on data obtained from recent earthquakes and general advances in engineering seismology, the new codes have become quite explicit and stringent. A comprehensive treatment of seismic earth pressures can be found in the FEMA 450 document *NEHRP Recommended Provisions for Seismic Regulations for New Buildings and Other Structures* (BSSC 2004), which has been updated as FEMA 750 (BSSC 2010). Both documents endorse the use of the M-O solution or the M-O solution as simplified by Seed and Whitman (1970) for "yielding walls" and the Wood (1973) solution for "nonyielding" walls. In this treatment, yielding walls are those that can translate, rotate, and/or deflect, such as typical gravity or cantilever walls, whereas nonyielding walls those that are stiff and "rigid," such as basement walls.

A review of the performance of basement walls in past earthquakes by Lew et al. (2010a) showed that failures of basement or deep-excavation walls in earthquakes are rare even if the structures were not explicitly designed for earthquake loading. Similarly, a review of the performance of various other retaining-structure types by Sitar et al. (2012) indicated that failures are relatively infrequent (e.g., Whitman 1991; Al-Atik and Sitar 2010; Sitar et al. 2012; Mikola 2012) and, when they occur, tend to be due to complex site conditions, such as sloping ground either above or below the retaining structure. Overall, there is no evidence of a systemic problem with traditional static retaining-wall design even under quite severe loading conditions (e.g., Gazetas et al. 2004). Most recently, no significant retaining-structure damage or failure occurred in the 2008 Wenchuan earthquake in China (Sitar et al. 2012) or in the great subduction earthquakes in Chile in 2010 (Verdugo et al. 2012) and in Japan in 2011 (Sitar et al. 2012). These observations are consistent with the conclusion reached by Seed and Whitman (1970), who

suggested that gravity retaining structures designed with an adequate factor of safety under static loading should perform well under seismic loading for PGA up to approximately 0.3g.

The most challenging aspect of evaluating the adequacy of existing methods of analysis is the fact that well-documented case histories with actual design and performance data for modern retaining structures are very sparse. A rare well-documented casehistory analysis of the performance of flood channel walls in the Los Angeles basin during the 1971 San Fernando earthquake was performed by Clough and Fragaszy (1977). They observed that reinforced-concrete cantilever structures, well designed and detailed for static loading, performed without any sign of distress at accelerations up to approximately 0.4g.

Given the paucity of reported failures of modern retaining structures in recent earthquakes in juxtaposition with increasingly stringent seismic design requirements, this research was undertaken to evaluate the adequacy of current design approaches. Specifically, this experimental program built on the work of Al Atik and Sitar (2010) and was aimed at evaluating the seismic behavior of rigid and flexible structures retaining cohesionless backfill. Cohesionless backfill was chosen to provide the most severe loading condition because it is rare in typical construction settings. The principal observations and findings of this experimental program are summarized herein; the complete details are presented in Mikola (2012); and the digital data are available from Mikola et al. (2013a, b).

Experimental Program

Two sets of centrifuge-scale experiments were carried out on the centrifuge at the Center for Geotechnical Modeling at UC Davis. A flexible shear-beam (FSB) container, consisting of a series of aluminum rings separated by neoprene layers, was used for the experiments. This container has dimensions of 1.65 m long × 0.79 m wide × 0.58 m deep. The seismic input is simulated by a servohydraulic shaking table, which is controlled by a conventional closed-loop feedback-control system and produces accelerations up to 30g at 200 Hz. The peak shaking velocity is approximately 1 m/s and the stroke is 2.5 cm peak to peak. To minimize boundary effects, the container was designed with a natural frequency smaller than that of a model soil deposit (Kutter 1995). The centrifugal acceleration used in the two experiments was 36g, and all results are presented in terms of prototype units unless otherwise stated.

Model Test Configurations and Preparation

The first centrifuge experiment, Rooz01, was performed on a uniform-density sand model. In prototype scale, the Rooz01 model consisted of two retaining-wall structures, stiff and flexible nondisplacing basement walls, of approximately 6 m in height and spanning the width of the container. The structures were designed to have the stiffness, mass, and natural frequency

of typical reinforced-concrete structures. They sat on approximately 12.5 m of dry medium-dense sand (Dr = 75%), and the backfill soil consisted of dry mediumdense sand (Dr = 75%). Both structures had stiff mat foundations. The second centrifuge experiment, Rooz02, was performed on a two-layer sand model. The Rooz02 model consisted of the nondisplacing U-shaped cantilever and displacing retaining-wall structures. The structures sat on approximately 12.5 m of dry medium-dense sand (Dr = 80%) and supported a dry medium-dense sand backfill (Dr = 75%). The model configuration is shown in Figs. 1(a and b) in model units in profile and plan views.

Structure Properties

Three different prototype retaining-structure types were modeled in this research effort as follows: (1) a nondisplacing cross-braced (basement) structure with a stem stiffness of 5.92 and a 1.04×1010 lb-in.2 per ft width; (2) a nondisplacing U-shaped cantilever structure with a stem stiffness of 5.92 and a 1.04×10^{10} lb-in.^{2} per ft width; and (3) a displacing retaining-wall with a stem stiffness of 2.4×10^{10} lb-in.^{2} per ft width. The terms *displacing* and *nondisplacing* are used here to differentiate structures by whether they can translate and/or rotate on their foundations during shaking. All of the retaining structures were constructed of T6061 aluminum plate [Young's modulus of 69,000 MPa (10,000 ksi) and Poisson's ratio of 0.32]. The nondisplacing basement wall consisted of two parallel plates braced by six threaded bars (three on the top and three on the bottom). To prevent the soil from heaving into the opening, a thick aluminum plate was added at the basement floor, which was set independent from the walls. The displacing cantilever wall consisted of a footing and a wall stem, bolted together as an inverted T. Likewise, the nondisplacing cantilever wall consisted of plates bolted to a thick footing as a U-shaped channel.

Instrumentation

Different instrument types were used in the experiments to record the models' seismic response. The main objective was to obtain a reliable measure of earth pressures and to characterize the ground motions. Thus, accelerometers were used to measure accelerations in the soil, the structures, and the container, and load cells were used to measure the axial load in the struts connecting the south and north walls of the basement. Additionally, soil settlement was measured at different locations with linear potentiometers (LPs) and the horizontal wall displacements were recorded with LVDTs placed in a special frame attached to the centrifuge bucket. Free Form Tactilus pressure sensors (SPI, Madison, New Jersey) were attached at the soil interface of the basement and cantilever walls. These sensors are 25.4 mm in diameter and 0.4 mm thick, which minimizes the stress arching around the sensor. To calibrate the pressure cells, the vertical stress γ^H was measured at the footing of the cantilever walls during spin-down at the end of the centrifuge experiment. Because Free Form Tactilus sensors are nonlinear resistances, the relationship between pressure and output voltage

is also nonlinear. Total bending moments were measured in the cantilever wall and the north basement wall with full-bridge strain gauges. The strain gauges were calibrated off the arm by fixing the wall at the footing and applying a strip load at the top. The high-speed data acquisition system used in the centrifuge collects data at 4,096 samples per second on every channel. For experiments with a scaling factor of $N = 36$, a typical input ground motion has frequencies between 10 and 300 Hz in model scale. The accelerometers and load cells had a frequency limit of 12,000 and 2,000 Hz, respectively, which is considered adequate to capture the frequencies of the seismic input motions. The displacement transducers, on the other hand, had an operating frequency of 20 Hz and were used only to measure static displacements. In the case of the Tactilus pressure sensors, the manufacturer indicates a maximum frequency response of 100 Hz; however, it was observed that the practical limit was actually in the range of 0–200 Hz. The locations of strain gauges and pressure transducers placed on the side walls of the retaining structures are shown in Figs. 2(a and b).
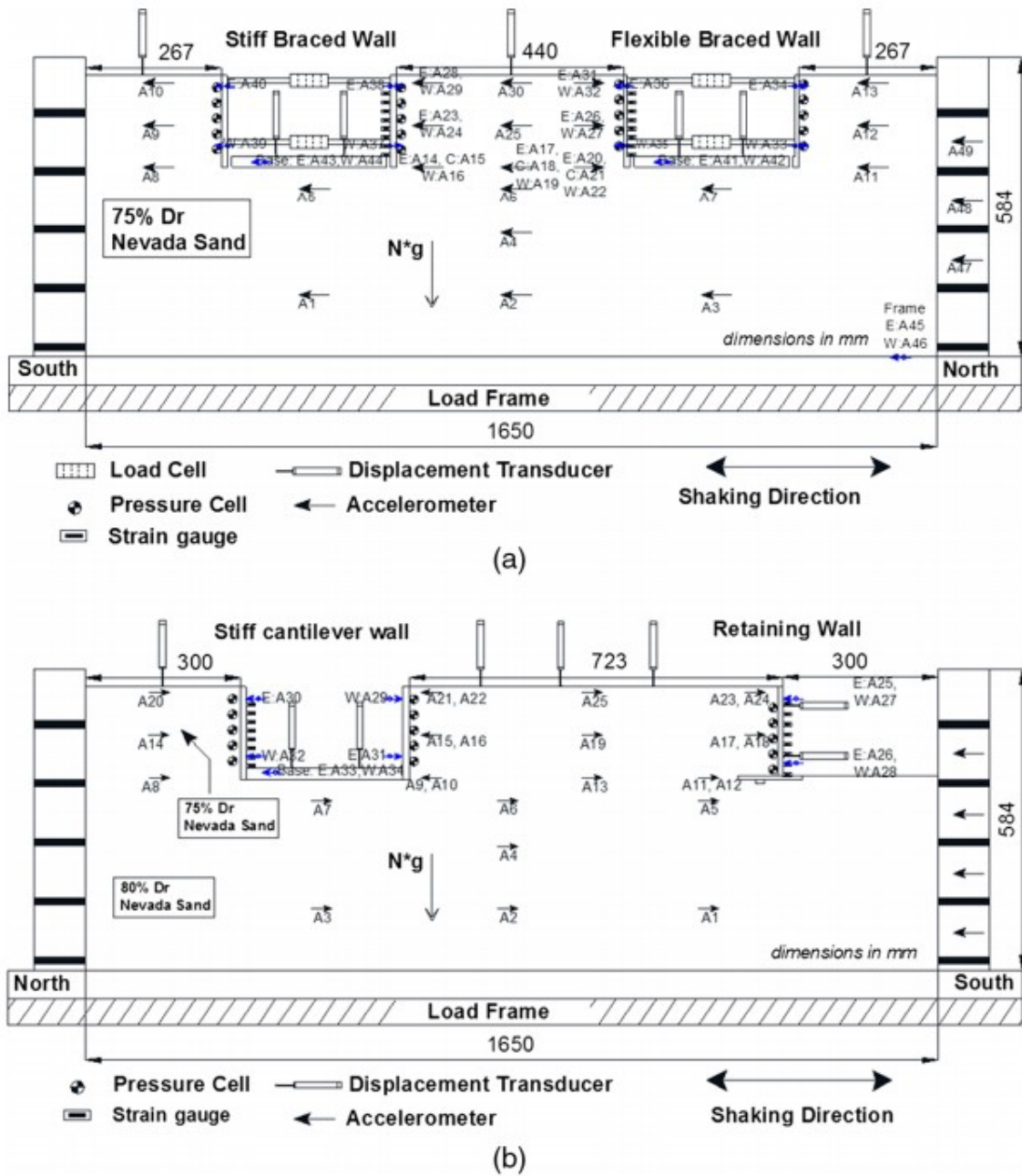
Fig. 1. Model configurations, profile view: (a) Rooz01; (b) Rooz02 (mm)

(a)   (b)

Fig. 2. (a) Strain gauges located at the walls of the retaining structures; (b) pressure transducers placed on the sides of the retaining structures

Input Ground Motions

Multiple shaking events were applied to the Rooz01 and Rooz02 models in flight at 36-*g* centrifugal acceleration. The shaking was applied parallel to the long sides of the model container and orthogonal to the model structures. The shaking events consisted of a step wave, a ground motion recorded at the Takatori (TAK) stations during the 1995 Kobe earthquake, applied two times, and at the Santa Cruz station during the Loma Prieta 1989 earthquake, applied once; and ground motions recorded at the Yarmica (YPT) station during the 1999 Kocaeli, Turkey, earthquake and at the Saratoga West Valley College (WVC) stations during the Loma Prieta 1989 earthquake. Step waves are usually applied at the beginning of a shaking series to test the instruments and the data acquisition system.

Table 1. Input Ground Motion Parameters for the Different Shaking Events in the Two Sets of Experiments

Test series	Shaking event	PGA (g)	I_a (m/s)	T_P (s)	T_m (s)	D_{5-95} (s)
Rooz01	Kobe-TAK090-1	0.69	4.13	0.19	0.52	6.27
	Loma Prieta-SC-1	0.41	0.97	0.35	0.62	10.79
	Kocaeli-YPT060-1	0.02	0.00	0.63	0.61	16.83
	Kocaeli-YPT060-2	0.11	0.06	0.62	0.60	6.39
	Kocaeli-YPT060-3	0.21	0.23	0.27	0.56	6.09
	Kocaeli-YPT330-1	0.07	0.03	0.23	0.62	6.98
	Kocaeli-YPT330-2	0.27	0.30	0.15	0.60	6.69
	Loma Prieta-WVC270-1	0.24	0.25	0.24	0.63	4.44
	Kocaeli-YPT330-3	0.24	0.28	0.27	0.66	7.75
	Kobe-TAK090-2	0.50	2.48	1.14	0.80	7.17
	Loma Prieta-WVC270-2	0.21	0.22	0.24	0.66	4.59
Rooz02	Kocaeli-YPT060-1	0.13	0.08	0.27	0.60	6.34
	Kocaeli-YPT060-2	0.14	0.10	0.27	0.58	6.45
	Kocaeli-YPT060-3	0.23	0.27	0.27	0.55	6.27
	Kocaeli-YPT330-1	0.26	0.36	0.23	0.57	6.73
	Loma Prieta-SC-1	0.39	1.09	0.35	0.59	10.97
	Kobe-TAK090-1	0.65	4.38	0.19	0.53	6.27
	Loma Prieta-SC-2	0.39	1.06	0.30	0.59	10.98
	Loma Prieta-WVC270-1	0.19	0.22	0.24	0.64	4.91
	Kocaeli-YPT330-2	0.24	0.34	0.23	0.58	6.97
	Kobe-TAK090-2	0.64	4.35	0.19	0.54	6.27

The input ground motion parameters are listed in Table 1. The peak ground acceleration of the input motions ranged from 0.02 to 0.69*g*, and the predominant period ranged from 0.15 to 1.14 s, thus spanning a broad range of ground motion characteristics. Input ground motions for experiments

Rooz01 and Rooz02 reasonably reproduced the range of frequencies seen in typical earthquakes. However, travel limitations of the shaking table limited the lowfrequency content of the input motions and therefore affected the overall spectra of the motions. It is significant that the peak acceleration in Table 1 is the peak horizontal acceleration measured at the base of the model container.

Experimental Results

Dynamic Earth Pressures

Direct measurement of lateral earth pressures using miniature pressure transducers was originally intended. However, because of the performance characteristics of these sensors, their use in this study was restricted to identifying behavioral trends and providing support for measurements obtained from strain gauges and load cells. Although there was some pressure drop at some of the pressure sensors during shaking events, overall observations indicated that seismic earth pressure increases monotonically with depth. In experiment Rooz01, the area underneath the dynamic pressure distribution given by the earth pressure transducers was corrected based on overall load estimated by the load cells and the corresponding linear pressure profiles were back-calculated (Fig. 3). To determine the dynamic earth pressure profiles from the strain gauge measurements, the maximum total moments at the base of the walls were extrapolated using the cubic polynomial fit and the corresponding linear pressure profiles that generated these moments were backcalculated. The maximum total pressure profiles interpreted from the strain gauge data were corrected to remove wall inertial effects and therefore represented dynamic earth pressure profiles (Fig. 3). Figs. 4 and 5 show the distribution of dynamic earth pressures recorded by the pressure sensors and interpreted from the load cells and strain gauges in the two series of experiments. Theoretical pressure distributions using the Mononobe-Okabe (M-O) and the Seed and Whitman (S-W) methods are shown as a reference and assume $K_h = 100\%$ PGA. The earth pressures are shown at the time of maximum dynamic moment, which does not necessarily correspond to the maximum observed earth pressure, as noted by Al-Atik and Sitar (2010). As shown in Fig. 4, the pressure sensors measured overall lower pressures than those interpreted from the strain gauges and load cells. All of the data points plotted in Fig. 4 were extracted at the exact same time.

Seismic Earth Pressure Distribution

The centrifuge data consistently show that for structures with heights between 6.1 and 9.15 m (20–30 ft), the maximum dynamic earth pressures increase with depth and can be reasonably approximated by a triangular distribution analogous to that used to represent static earth pressures. This result is contrary to the assumption of Seed and Whitman (1970), which was based on experiments by Matsuo (1941) and other similar shaking-table experiments. Matsuo's experiments were on dry, relatively loose sand on a

rigid shaking table and retaining walls up to 1.8 m (6 ft) high. Although these experiments were performed meticulously and were pioneering in their scope at the time, they cannot be simply scaled to capture the response of taller structures. More important, the observed amplification of ground motion and the observed increase in earth pressure against the wall at the free surface appear to be direct results of the physical layout of the model geometry, the shaking-table box, and the properties of the sand. In that sense, Matsuo's results are correct for the given geometry and material and thus are directly applicable to walls up to 1.8 m (6 ft) high with relatively loose granular backfill.

Dynamic Wall Deflections in the Centrifuge Tests

The minimum active pressure acting on a wall occurs when the wall moves sufficiently far outward for the soil behind it to expand laterally and reach a state of plastic equilibrium. The amount of movement necessary to reach these conditions depends primarily on the type of backfill material, as shown in Table 2 (Canadian Geotechnical Society 1992). For a rigid wall that is free to translate or rotate about its base, the active or passive condition occurs if sufficient movement can take place and the pressure distribution remains approximately triangular.
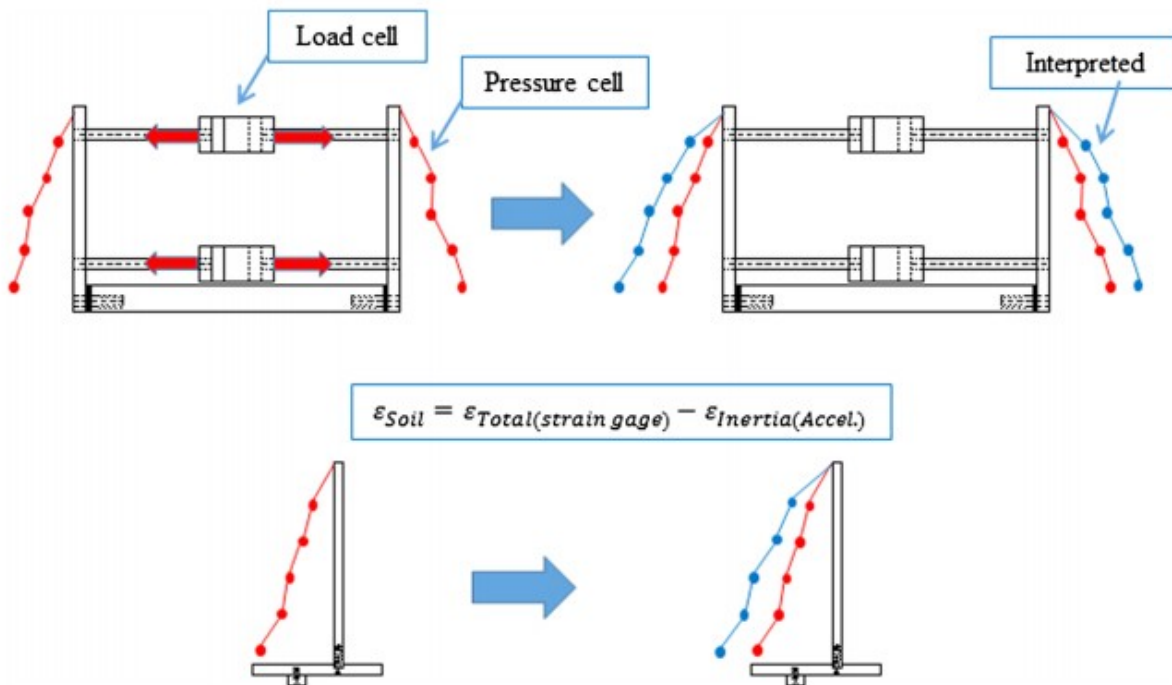

$$\varepsilon_{Soil} = \varepsilon_{Total(strain\,gage)} - \varepsilon_{Inertia(Accel.)}$$

Fig. 3. Procedure used to interpret the earth pressure measured by the pressure transducer
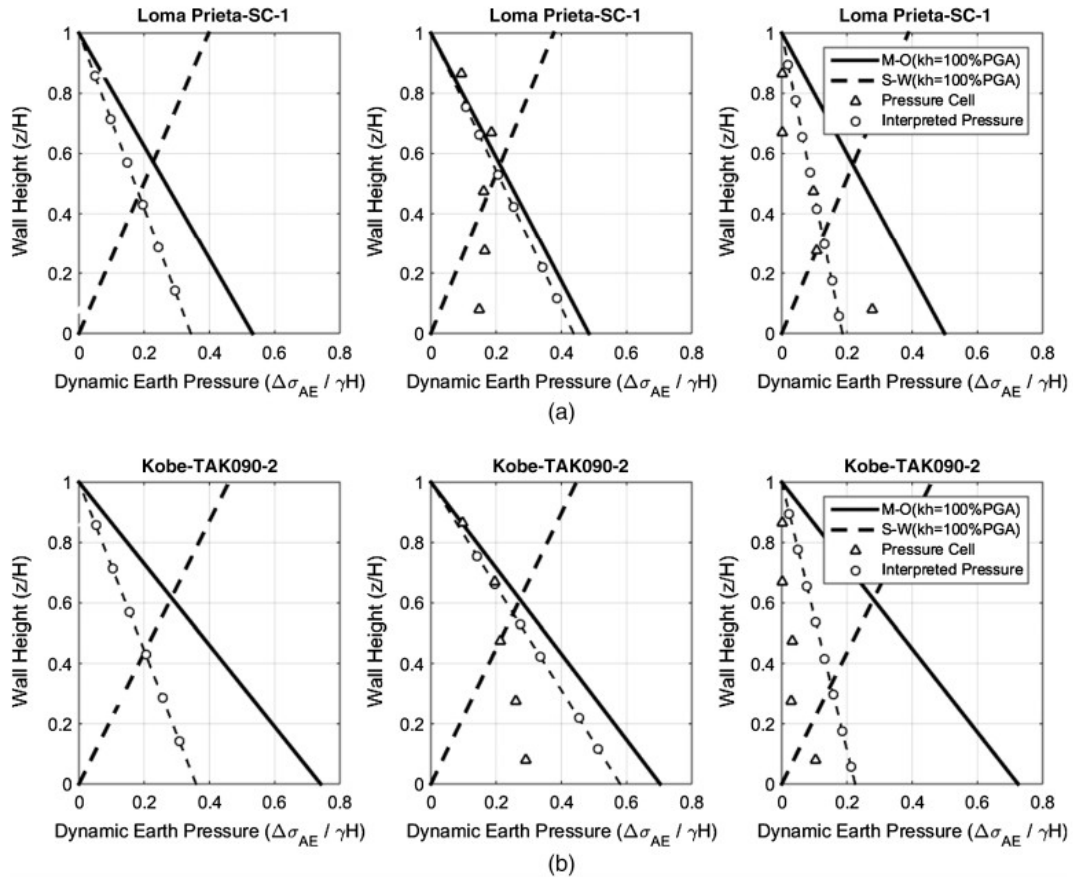
Fig. 4. Dynamic earth pressure distributions measured directly and interpreted from the pressure sensors and strain gauge, load cell data, and estimated M-O and S-W on walls for (a) Loma Prieta-SC-1 (PGA$_{ff}$ = 0.51g); (b) Kobe-TAK090-2 (PGA$_{ff}$ = 0.61g)

Figs. 6 and 7 show the rigid body translation and transient deflection of both the nondisplacing cantilever and the displacing retaining walls derived from LVDT and strain gauge measurements in the experiments.

As can be seen, the transient deflection measured by the strain gauges passed the necessary displacement (i.e., 0.001H) to produce active earth pressure after 0.3 free-field PGA. In case of the displacing cantilever wall (Fig. 6), the rigid body translation data show significantly more scatter compared with transient deflection because there is a significant amount of settlement as the sand densifies when subjected to the first several low-amplitude events. The transient deflections, on the other hand, follow a consistent trend of increasing with increasing free-field PGA, as shown in Figs. 6 and 7.
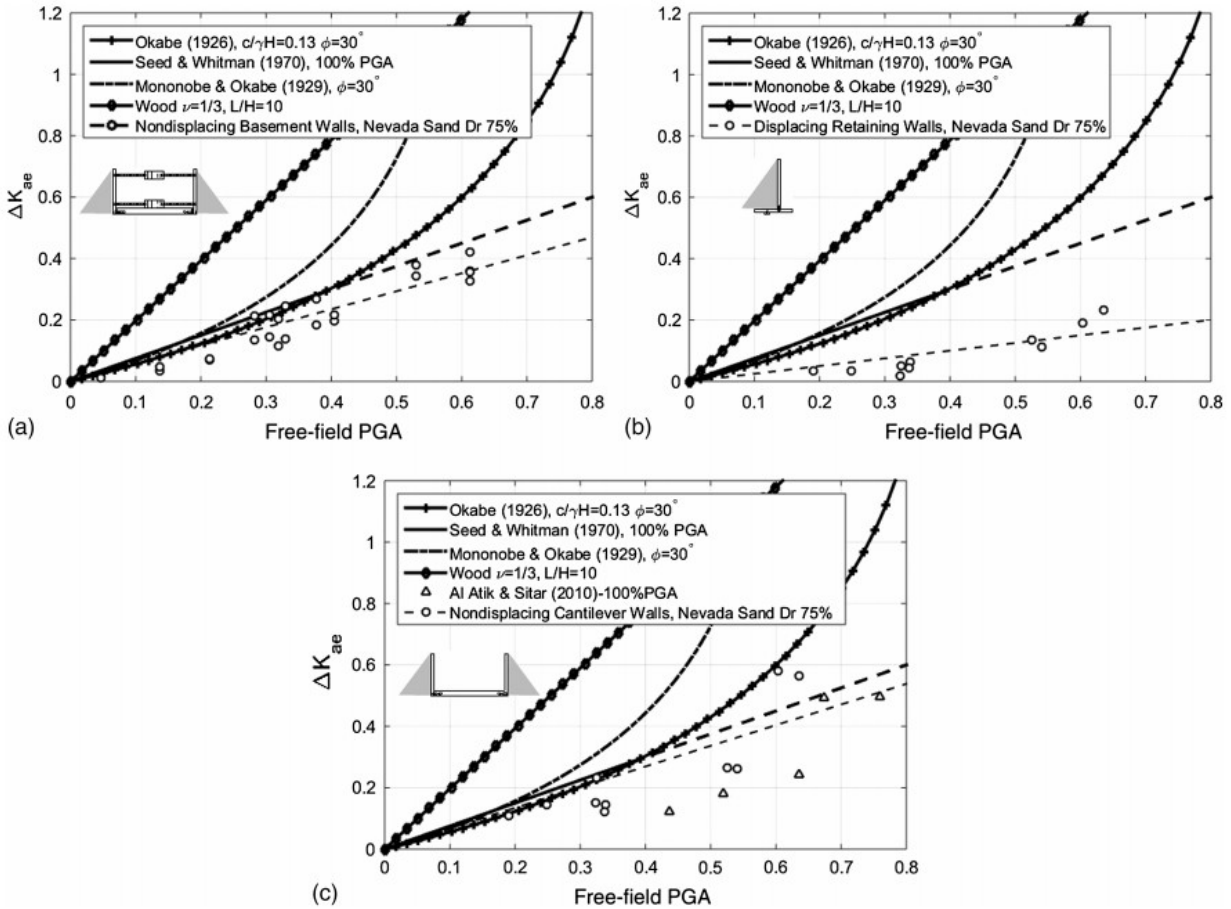
Fig. 5. Back-calculated dynamic earth pressure coefficients at the time of maximum dynamic wall moments and maximum dynamic earth pressures on (a) nondisplacing basement wall; (b) displacing retaining wall; (c) nondisplacing U-shaped cantilever wall

Table 2. Wall Displacements Required to Develop Active and Passive Earth Pressures (Data from Canadian Geotechnical Society 1992)

Soil type and condition	Value of Δ/H	
	Active	Passive
Dense cohesionless	0.001	0.02
Loose cohesionless	0.004	0.06
Stiff cohesive	0.010	0.02
Soft cohesive	0.020	0.04

Effect of the Static Factor of Safety

In accordance with allowable static lateral earth pressure, it is common practice to calculate the design capacity (allowable earth pressure) of a retaining wall by applying a factor of safety (FS) to the ultimate static force. The purpose of the FS is to incorporate the combined effect of various factors, including, but not limited to, the variability of the soil, the lack of confidence in developing input parameters such as soil properties, the construction control, and the limitations of the method used for estimating the ultimate capacity. The design and allowable capacity of the retaining wall
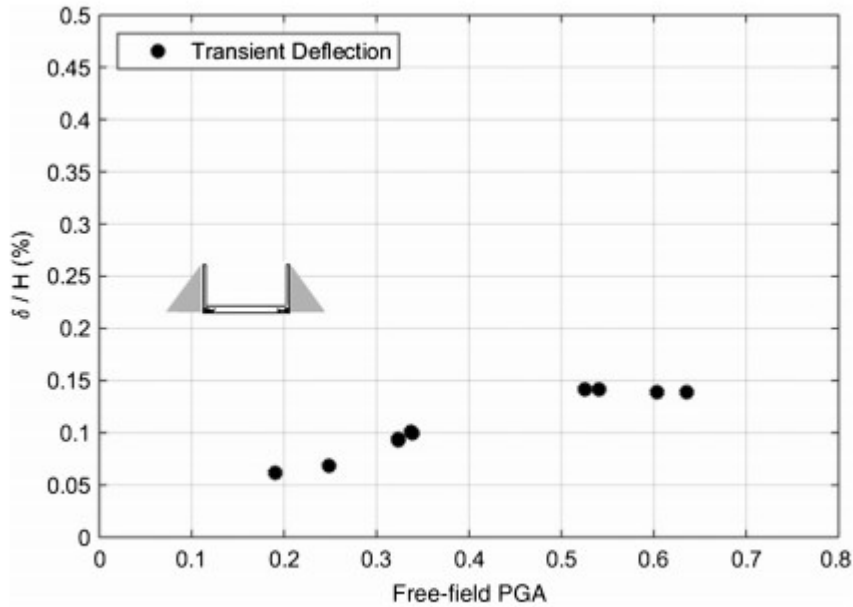
can be calculated by $Q_{allowable} = Q_{ult}/FS$. The Coulomb lateral earth pressure theory gives the resultant static force acting on the retaining wall as (allowable capacity): $P_{static} = 1/2\ K_h\gamma H^2$, where P_{static} is the lateral earth pressure result; K_h is the lateral earth pressure coefficient; γ is the unit weight of the backfill; and H is the wall depth. The value of K_h used for design depends on the soil properties and the displacement of the structure (i.e., whether the backfill is at rest, active, or passive). Thus, the design capacity can be expressed as

$$Q_{ult} = \left(\frac{1}{2}K_h\gamma H^2\right) \times FS \qquad (1)$$

This equation can be recast to reflect the design load with a factor of safety of 1 (FS = 1) and an additional design load due to the added margin of safety; thus

$$Q_{ult} = \left(\frac{1}{2}K_h\gamma H^2\right) + \left(\frac{1}{2}K_h\gamma H^2\right) \times (FS - 1) \qquad (2)$$

The second term of Eq. (2) can be interpreted in terms of the dynamic earth pressure increment, as suggested by Seed and Whitman (1970).

Fig. 6. Transient deflection and rigid body translation of the displacing cantilever wall

Fig. 7. Transient deflection of the nondisplacing retaining wall

Fig. 8 shows the plot of static design capacity versus free-field PGA for both nondisplacing and displacing walls for an assumed factor of safety of 1.5. A typical factor of safety might be used to design retaining walls to resist sliding and overturning. In general, however, the overall FS is higher because of an accumulation of FSs at different stages of design; therefore, it might significantly exceed 1.5 depending on the level of confidence in the geotechnical design. These plots show that, at PGA values less than 0.3, the dynamic earth pressure increment does not exceed the static design capacity for a design with a static FS of 1.5 for both nondisplacing basement walls and nondisplacing U-shaped cantilever structures. This effect is even more pronounced for free-standing cantilever structures.
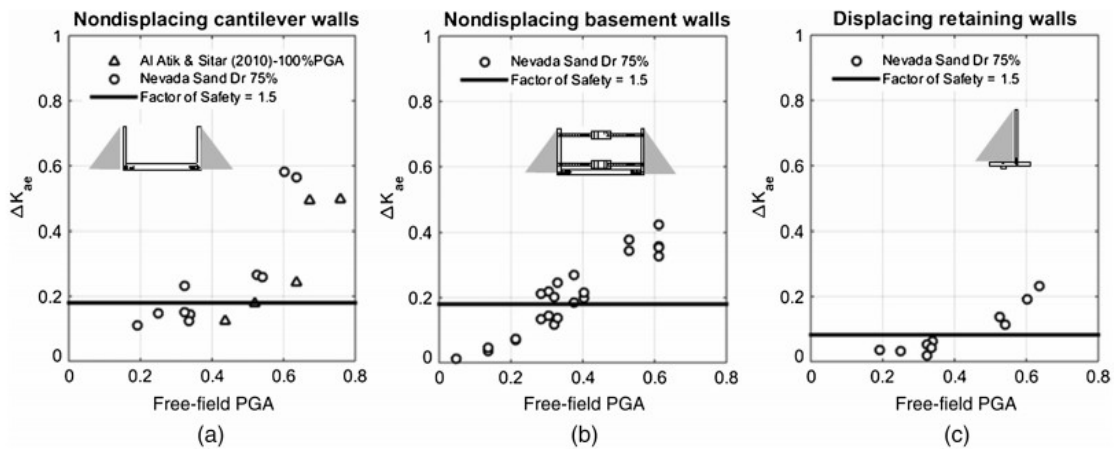
Fig. 8. Dynamic earth pressure coefficient and static design capacity for a design with static FS = 1.5 as a function of PGA for (a) nondisplacing U-shaped cantilever walls; (b) nondisplacing basement walls; (c) displacing retaining walls

These conclusions are consistent with those of Seed and Whitman (1970), who observed that a wall designed to a reasonably static FS should resist seismic loads of up of 0.3g. They are also consistent with the observations and analyses performed by Clough and Fragaszy (1977) and Al-Atik and Sitar (2010), who concluded that conventionally designed cantilever walls with granular backfill can be expected to resist seismic loads at accelerations up to 0.4g.

Conclusions

The data show that seismic earth pressure increments increase with depth consistent with the static earth pressure distribution and consistent with that implicit in the M-O solution which forms the upper bound for the experimental results. The overall trends in the incremental dynamic earth pressures data show that the Seed and Whitman (1970) approximation using PGA represents a reasonable upper bound for the value of the seismic earth pressure increment for both fixed-base cantilever structures (U-shaped walls) and cross-braced basement-type walls. In comparison, the M-O solution and the Mylonakis et al. (2007) solutions are considerably higher than the measured values at accelerations above approximately 0.4g. The equivalent Wood (1973) seismic earth pressure, computed using the prototype structure dimensions, clearly exceeds all other results by a considerable margin, as expected based on the assumptions used in this solution. The Seed and Whitman (1970) solution with PGA produces a reasonable upper bound over a range of experimental results for both nondisplacing cantilever and cross-braced U-shaped structures. The use of 0.85 PGA in the same analysis produces values very close to the mean of the experimental data. In contrast, the dynamic earth pressure increments on free-standing cantilever walls are significantly smaller and correspond to using 0.35 PGA in the Seed and Whitman approximation. All of these issues deserve further careful evaluation because the costs of an overconservative design can be just as much of a problem as the cost of a future failure.

Direct measurement of lateral earth pressures using miniature pressure transducers was originally intended. However, because of the performance characteristics of these sensors, the use of load cells in the basement wall and strain gauges in the cantilever wall was necessary to evaluate the magnitude of the seismic loads. For future studies, the pressure transducers with high-accuracy responses are clearly desirable, if not essential, to directly measure the dynamic earth pressure magnitude and its distribution.

Finally, it is significant that the results in this study strictly apply to dry cohesionless medium-dense materials with a certain wall height (6.1–9.15 m). At this point, more experimental work and well-documented case histories are needed to fully explore the range of potential soil conditions and retaining-structure types. In particular, there is a need for the development of a database of field observations from instrumented sites and

structures to verify the analysis and design assumptions and to develop the most cost-effective designs.

References

Aitken, G. H. (1982). "Seismic response of retaining walls." M.S. thesis, Univ. of Canterbury, Christchurch, New Zealand.

Al Atik, L., and Sitar, N. (2010). "Seismic earth pressures on cantilever retaining structures." J. Geotech. Geoenviron. Eng., 10.1061/(ASCE) GT.1943-5606.0000351, 1324–1333.

BSSC (Building Seismic Safety Council). (2004). NEHRP recommended provisions for seismic regulations for new buildings and other structures (FEMA 450): Part 1—Provisions, Washington, DC.

BSSC (Building Seismic Safety Council). (2010). NEHRP recommended provisions for seismic regulations for new buildings and other structures (FEMA 750): Part 1—Provisions, Washington, DC.

Canadian Geotechnical Society. (1992). Canadian foundation engineering manual, 3rd Ed., BiTech Publishers, Richmond, BC.

Clough, G. W., and Fragaszy, R. F. (1977). "A study of earth loadings on floodway retaining structures in the 1971 San Fernando Valley earthquake." Proc., 6th World Conf. on Earthquake Engineering, Vol. 3, Indian Society of Earthquake Technology, India.

Gazetas, G., Psarropoulos, P. N., Anastasopoulos, I., and Gerolymos, N. (2004). "Seismic behaviour of flexible retaining systems subjected to short-duration moderately strong excitation." Soil Dyn. Earthquake Eng., 24(7), 537–550.

Kutter, B. L. (1995). "Recent advances in centrifuge modeling of seismic shaking." Proc., 3rd Int. Conf. on Recent Advances in Geotechnical Earthquake Engineering and Soil Dynamics, Vol. 2, St. Louis, 927–941.

Lew, M., Sitar, N., and Al Atik, L. (2010a). "Seismic earth pressures: Fact or fiction." Earth Retention Conf., ER 2010, ASCE, Seattle.

Lew, M., Sitar, N., Al Atik, L., Pourzanjani, M., and Hudson, M. B. (2010b). "Seismic earth pressures on deep building basements." Proc., 79th Annual Convention, Structural Engineers Association of California, Indian Wells, CA.

Matsuo, H. (1941). "Experimental study on the distribution of earth pressures acting on a vertical wall during earthquakes." J. Jpn. Soc. Civ. Eng., 27(2), 83–106.

Mikola, G. R.. (2012). "Seismic earth pressures on retaining structures and basement walls in cohesionless soils." ⟨http://escholarship.org/uc/item/8rm5s4dw⟩.

Mikola, R. G., Candia, G., and Sitar, N. (2013). "Seismic earth pressures on braced wall in sand (Rooz01)." Network Earthquake Eng. Simul. (Distributor), Dataset.

Mikola, R. G., Candia, G., and Sitar, N. (2013a). "Seismic earth pressures on braced wall in sand (Rooz01)." Network Earthquake Eng. Simul. (Distributor), Dataset, in press.

Mikola, R. G., Candia, G., and Sitar, N. (2013b). "Seismic earth pressures on non-displacing and displacing retaining wall in sand (Rooz02)." Network Earthquake Eng. Simul. (Distributor), Dataset, in press.

Mononobe, N., and Matsuo, M. (1929). "On the determination of earth pressures during earthquakes." Proc., World Engineering Conf., Vol. 9, 177–185.

Mylonakis, G., Kloukinas, P., and Papatonopoulos, C. (2007). "An alternative to the Mononobe-Okabe equation for seismic earth pressures." Soil Dyn. Earthquake Eng., 27(10), 957–969.

Nazarian, H. N., and Hadjian, A. H. (1979). "Earthquake induced lateral soil pressures on structures." J. Geotech. Eng. Div., 105(GT9), 1049–1066.

Okabe, S. (1924). "General theory on earth pressure and seismic stability of retaining wall and dam." J. Jpn. Soc. Civ. Eng., 10(6), 1277–1323.

Prakash, S. (1981). "Dynamic earth pressures." State of the Art Rep.– Int. Conf. on Recent Advances on Geotechnical Earthquake Engineering and Soil Dynamics, Vol. 3, Univ. of Missouri-Rolla, MO, 993–1020.

Prakash, S., and Basavanna, B. M. (1969). "Earth pressure distribution behind retaining wall during earthquakes." Proc., 4th World Conf. on Earthquake Engineering, Chilean Association on Seismology and Earthquake Engineering.

Seed, H. B., and Whitman, R. V. (1970). "Design of earth retaining structures for dynamic loads." ASCE Specialty Conf., Lateral Stresses in the Ground and Design of Earth Retaining Structures, Cornell Univ., Ithaca, NY, 103–147.

Sitar, N., Mikola, R. G., and Candia, G. (2012). "Seismically induced lateral earth pressures on retaining structures and basement walls." GeoCongress 2012, Geotechnical Engineering State of the Art and Practice, Oakland, CA, 335–358.

Verdugo, R., et al. (2012). "Seismic performance of earth structures during the February 2010 Maule, Chile, earthquake: Dams, levees, tailings dams, and retaining walls." Earthquake Spectra, 28(S1), S75–S96.

Whitman, R. V. (1991). "Seismic design of earth retaining structures." Proc., 2nd Int. Conf. on Recent Advances in Geotechnical Earthquake Engineering and Soil Dynamics, ASCE, St. Louis, 1767–1778.

Wood, J. H. (1973). "Earthquake induced soil pressures on structures." Ph.D. thesis, California Institute of Technology, Pasadena, CA.